Evidence of cosmic recurrent & lagged millennia-scale patterns and consequent forecasts: Multi-scale responses of solar activity (SA) to planetary gravitational forcing (PGF).

J. Sánchez-Sesma[1,2]

[1]{Instituto Mexicano de Tecnología del Agua, Mexico}

[2]{Now independent consultant, Mexico}

Correspondence to: J. Sánchez-Sesma (jorgesanchezsesma@yahoo.com)

Abstract

Solar activity (SA) oscillations over the past millennia are analyzed and extrapolated based on reconstructed solar-related records. Here, simple recurrent models of SA signal are applied and tested. The consequent results strongly suggest: a) the existence of multi-millennial (~9500-yr) scale solar patterns linked with planetary gravitational forcing (PGF), and b) their persistence, over at least the last glacial-interglacial cycle, but possibly since the Miocene (10.5 Ma). This empirical modelling of solar recurrent patterns has also provided a consequent multi-millennial-scale experimental forecast, suggesting a solar decreasing trend toward Grand (Super) Minimum conditions for the upcoming period, 2050-2250 AD (3750-4450 AD). Taking into account the importance of these estimated SA scenarios, a comparison is made with other SA forecasts. In two Appendixes, we provide further verification, testing and analysis of solar recurrent patterns since geological eras, and their potential gravitational forcing.

Keywords

Solar activity, millennia-scale, patterns, forecast, planetary forces, gravitational forcing, multi-scale, lagged response

1 Introduction

“Long-term solar variability: It is possible that we have missed the forest for the trees. Driven by pragmatic hopes of finding keys to weather prediction, we run the risk of concentrating too much on time scales of practical consequences -- of days, months or years. In taking a longer view we see the problem in clearer perspective… "

Climate and the Role of the Sun (John A. Eddy, 1981)

Solar activity (SA) has non-linear characteristics that influence multiple scales in solar processes (Vlahos and Georgoulis, 2004). For instance, millennia-scale solar oscillations have been recently detected, like those of about 6000 and 2400 years, by Xapsos and Burke (2009) and Charvátová (2000), respectively, with important and interesting influences in the near past and future climate. These millennial-scale patterns of reconstructed SA variability could justify epochs of low activity, such as the Maunder Minimum, as well as epochs of enhanced activity, such as the current Modern Maximum, and the Medieval Maximum in the 12th century.

Although the reason for these SA oscillations is unclear, it has been proposed that they are due to chaotic behavior of non-linear dynamo equations (Ruzmaikin, 1983), or stochastic instabilities forcing the solar dynamo, leading to on-off intermittency (Schmitt et al., 1996), or planetary gravitational forcing with recurrent multi-decadal, multi-centennial and longer patterns (Fairbridge and Sanders, 1987; Fairbridge and Shirley, 1987; Charvátová, 2000; Duhau and Jager, 2010; Perry and Hsu, 2000). It should be noted that all proponents of planetary forcing have forecasted a solar Grand Minimum for the upcoming decades, but one of them has also forecasted a Super Minimum for the next centuries (Perry and Hsu, 2000). In addition, during recent decades, statistical forecasts (with physically-based spectral information of reconstructed records) of solar magnetic activity predict a clear decrease in SA, reaching a minimum around 2100 AD (Steinhilber et al., 2013; hereafter S13; Velasco et al., 2015).

It should also be noted that several recent studies have been devoted to reconstruct multi-millennial-scale solar/climate related records. In relation to solar records, Steinhilber et al. (2009; hereafter S09), Steinhilber et al. (2012; hereafter S12), Solanki et al. (2004; hereafter S04), and Finkel and Nishiizumi (1997; hereafter FN97) have investigated isotopic concentrations in ice-cores and tree-rings over the past 9,500, 9,500, 11,500, and 40,000 years, respectively, in order to estimate SA and/or related isotopic production. Another two isotopic reconstructions by Stuverik-Storm et al. (2014; hereafter SS14) and Adolphi et al. (2014; hereafter A14) have just provided detailed key information over 20 Kyrs for the past interglacial, or Eemian, more than 100,000 years ago, and for the last deglaciation, over 8Kyr from 19 to 11 Kya, respectively.

These different cosmogenic radionuclide-based reconstructions of SA present variations for the past millennia, and as Muscheler and Heikkilä (2011) have pointed out, large uncertainties appear in reconstructions of the solar modulation of galactic cosmic rays from different proxies, 10Be and 14C, and of changes in the geomagnetic shielding influence. However, these reconstructed records provide, especially when considered all together, the most objective information as elements for detecting and eventually modelling and extrapolating multi-millennial-scale solar oscillations, trends and absolute levels.

In this work, we attempt to advance our knowledge of solar variability by considering reconstructed records of variables related with SA over the last glacial cycle, from isotopic information coming from ice-cores and tree-ring layers, reanalyzing them with a linear modelling of oscillations with recurrent influences. This modelling is achieved through simple analogues and Fourier series models. Tests of the proposed method and the detected low-frequency solar signal, going back in time, are based on independent data. Finally, we discuss the different oscillations detected, the confidence of our forecasts, some alternative forecast methods, and astronomical information that suggests a possible planetary gravitational forcing of SA by an unknown mechanism during the last millennia. Further analysis is provided in two Appendixes. Appendix A: Qualitative verification of total solar irradiance (TSI) ~9.5Ky recurrent patterns with a bivalve population (BVp) reconstructed from late Miocene (~10.5Mya) data; and Appendix B: Empirical evidence of a lagged planetary gravitational forcing of the ~9500yr total solar irradiance (TSI) recurrent pattern.

2 Methodology

2.1 Data

In order to analyze SA recurrent oscillatory patterns, different reconstructed forcing records of these oscillations are used.

We have analyzed five different sets of solar-related information. Firstly, total solar irradiance (*TSI* or *S*, hereafter) reconstructed by S04, S09 and S12, based on the isotopic information of ^{14}C and ^{10}Be, have recently provided records of SA anomalies for the last millennia. Figure A displays S04, S09 and S12 reconstructed and intercalibrated values from 9450 BC to 1900 AD, from 7360 BC to 2009 AD, and from 7350 BC to 1988 AD, respectively. The variance explanation (obtained as the square of the correlation coefficient multiplied by 100) between S04&S09, S04&S12, and S09&S12 for decadal average records are of 52.7, 82.9 and 59.3 %, respectively.

Secondly, there are three interesting and useful solar-related, 10Be isotope concentration records from Greenland ice core, one covering the past 40 Kyrs (FN97), another covering only 20 Kyrs but belonging to the Eemian (SS14), and another covering 20-10 Kyrs BP (A14). Figure 1b and Figure 1c display the information of 10Be reconstructed records by FN97, SS14, and A14.

2.2 Modelling

To take into account different time-scale recurrences, the solar/climate, *SC*, variable can be expressed with two models. One model is based on the Fourier Series (FS), another is based on a linear transformation of the proxy variable values, and the last one is based on temporal analogues.

The FS model can be written by means of:

$$SC(t) = \sum_{j=1}^{N_{FS}} \left[a_j \cdot \sin\left(j \frac{2\pi(t\ )}{T} \right) + b_j \cdot \cos\left(j \frac{2\pi(t\ )}{T} \right) \right] + e_{FS}(t)\,, \tag{1}$$

Here, T is the FS base period, N_{FS} represents the number of FS terms or harmonics, j is an index component term, a and b are amplitudes, t is time, and $e_{FS}(t)$ is the error in this model.

The analogue model is defined as:

$$SC(t) = \alpha_A SC(t+\delta_A) + \beta_A(t - t_1) + \gamma_A + e_A(t)\,, \tag{2}$$

Here, α_A is the amplification factor, β_A is the slope, δ_A is the lag, γ_A is the additive constant, t_1 is the initial times for the modeled period, and $e_A(t)$ is the analogue error of this model.

In all these models, parameters are estimated through iterative or multi-linear regression processes that minimize the RMS values of errors.

Taking into account both the dating limitations and the approximated values provided by proxy reconstructions, and instead of developing statistical analysis, as convergence and confidence level estimations, we prefer in this stage of research on solar climate recurrences, to apply verification/replication of all of our findings with independent information in our estimation processes and results. Future climate reconstructions with more accurate information will provide further and refined statistical analysis.

3 Results

3.1 Long-term solar-activity recurrent patterns

In order to detect multi-millennia-scale recurrences and/or persistent oscillations in SA, we need to analyze 10Be information since it is a solar proxy variable and it is available over longer periods than SA records (SS14). However, there are several 10Be post-production and fallout processes (i.e. residence time in the atmosphere, scavenging rate, troposphere-stratosphere exchange, precipitation rate, etc.) that may alter the concentration found in the ice archive (FN97; SS14).

Accepting that 10Be concentration variability is influenced by climatic variability through long-term variable trends and modulations, we propose to apply a homogenization process based on statistics to the 10Be (FN97) record. Firstly, a detrending process based on polynomial expressions was applied. And secondly, a demodulation was applied in an attempt to make the variance uniform. The consequent results show the 10Be atmospheric signal of this process with approximated recurrent oscillations with lags of 9.6 and 19.2 Kyrs, which are shown in the Supplementary Information (SI) Section 1 (SI-1).

The statistically detrended 10Be FN97 record was modeled with a periodic FS function with N_{FS}=10 that employed Eq. 1. After a minimization processes, a 9390 yr period, P, was found and the corresponding model that explain 49.2 % of variance is displayed in Figure 2a.

It should be noted that the solar and climate recurrence periods evaluated with FS and analogue techniques (shown in SI) have shown values of 9500+/-100 yrs (~9.5 Kyr).

Before extrapolating the 10Be ~9.5 Kyr recurrences to TSI, we applied a wavelet analysis to the three TSI records. The TSI spectral results (see SI-4) show three main, significant periodicities around 5000, 2400 and 900 years, and confirms the existence in solar activity of at least three harmonics of the ~9.5 Kyr oscillations.

3.2 Verification of the recurrences of 10Be ~9.5Ky patterns

Although this FS periodic 10Be model is based only on the last 40 Kyrs (see Figure 2b), it was extrapolated to cover the last 130 Kyrs, for comparison with other independent information of 10Be. A detailed comparison with the 10Be SS14 record (in 5 parts) coming from Greenland and the Eemian is displayed in Figure 2c. The maximum variance explanation, of 18.4%, corresponds to a temporal adjustment of 2.5 Kyrs (a temporal bias going back in time) of the SS14 dating. This temporal adjustment is justified because a similar one, of 2.3 Kyr, is required by the SS14 18O record when it is compared with another reconstruction from NGRIP Greenland ice-cores by Kindler et al. (2014; hereafter K14), which is shown in SI-2. This comparison constitutes an important verification and test of the proposed FS model.

In order to verify the detected recurrent patterns of 10Be, we apply different homogenization and extrapolation processes to FN97 data. Specifically, we follow the original calculations made by FN97 and the suggestions provided by Dr. Nishiizumi (personal communication, 2014), and we have also calculated the atmospheric signal of 10Be (10BeAtm) based on accumulated snow (Cuffey and Clow, 1997) and the signal of 10Be coming from the GISP2 ice core. Our normalizations, which are devoted to eliminating high-frequency local climate influences on the 10Be signal, have provided elements (records) to confirm the previous results for the ~9.5 Kyr recurrence and a consequent increase and diminishing of the 10BeAtm and TSI signals, respectively, for the following centuries, as also shown in the SI-3.

We have also shown, in Appendix A, a qualitative verification of the total solar irradiance (TSI) ~9.5Ky recurrent patterns with a bivalve population (BVp) reconstructed from late Miocene (~10.5Mya) data by Harzhauser et al. (2013). They developed a comparison, in the frequency domain, of their reconstruction, BVp, with solar activity, or TSI, (BVp, TSI) and found significant oscillations with periods from 20 to 200 yrs. Motivated by their findings, in an independent effort, we have developed the same comparison (BVp, TSI), but realized in the time domain over the complete 8000 yr record, with an extrapolated and adjusted TSI pattern. Thus, our comparison was in a different domain, the time domain, which considered all the range of oscillations.

3.3 Empirical tests of the recurrence and potential mechanisms of TSI ~9.5Ky patterns.

Looking for physical basis and robust evidence of the detected recurrences, we have developed two qualitatively different tests of the multi-millennial recurrences of TSI: a test based on a suggested gravitational forcing, and a test based on the TSI (S04) and 10Be (A14) records.

The first test, based on a physical mechanism, which develops a gravitational forcing analysis, is shown in Appendix B. It is an empirical analysis of gravitational forcing due to lateral forces. Those lateral forces generate a low-frequency signal with a period of ~9500 yrs, preceding by ~6700 yrs, and is similar to low-frequency solar activity. Additional analysis of a non-linear lagged response of TSI to gravitational forcing is developed and suggests a logarithmic model variation for different gravitational forcing periods.

The second test, which is based on a high-resolution independent and normalized 10Be record (A14), consists of an extrapolation backward in time of the TSI(S04) record [this record reconstructed sun-spot numbers or SSN], which is based on 14C records. Although 14C records are coming from well-dated tree-ring studies, a temporal bias correction of a 70-yr lead was applied to the 14C based TSI(S04) original record, before being extrapolated backward in time. This lead adjustment of 14C records is justified, to compensate their limitations, because these records are influenced by the global carbon cycle, causing fluctuations of the atmospheric ^{14}C concentration measured as $\Delta^{14}C$ in tree rings to be damped, smoothed and delayed relative to the ^{14}C production (S12).

After this important adjustment, an application of the analogue model (a linear leaded transformation with corrected trend), Eq. (2), produces an excellent agreement between the 14C based TSI(S04) record of SSN, with a lead of 9400 yrs, with TSI(10Be[A14]) record, displayed in Fig. 3.

3.4 Application of the ~9500 yr recurrence of SA

We applied equation 2 with a lag parameter of 9600 yrs to the TSI records, maximizing the match between the analogue model based on S04 information and the original S04 records.

Only the S04 model continually covers the next centuries, due to its longest characteristics, and presents an overlapping that explains 16% and 53.4% of the TSI variance of the last 1000 and 500 years, respectively. Results of TSI are displayed in Fig. 4. In this Figure, the three TSI records (S04, S09 and S12) are displayed with their analogue models.

However, in order to test the proposed method, we compare our TSI forecasts with a forecast for the next 500 yrs based on S12 data and the Fast Fourier Transform (FFT) techniques developed by S13. The TSI(S04) extrapolation explains 61.4% of the variance of the forecasted TSI(S13) which is based on other data and other technique. This comparison constitutes other important verifications and test of the proposed recurrent model of SA.

Our model confirms a Grand minimum in the period from 2050 to 2200 AD forecasted by S13, showing a sustained deficit of 0.5 W/m2, similar to that shown in the Maunder Minimum, four centuries ago (see Fig. 4b).

The same model, shown in Figure 3a, suggests that the next Super-minimum of SA will ocurr from -2100 to -2600 BP (4050-4550 AD), and will be similar to the period 7500-7000 BP of reduced SA. Please note, that in Figure S1, based only on 10Be, an experimental forecasted decrease of TSI is shown with a SA Super-minimum from -2 to -2.5 Kyr BP (3950 to 4450 AD). In Fig. 3, big and small vertical orange arrows indicate, the verified forecasts of Super and Grand solar minima, respectively.

4 Discussion

Firstly, and in order to confirm this multi-millennial recurrence, we have developed different tests and verifications of the SA recurrent patterns. In the following a summary of the tests and verifications of our findings is presented:

A. Our FS model explains the detrended and modulated 10Be statistically corrected variability over almost the last 40 Kyrs. However the recurrent patterns based on FN97 when extrapolated backward in time are comparable with independent 10Be information from the Eemian.

B. When this recurrent phenomena detected in the 10Be record was extrapolated to the TSI records, we conducted other tests, establishing the following: a) the overlapping of the TSI(S04) record explains over *53%* of the variance in the last five centuries; and b) the extrapolated model also based on TSI(S04) presents an important match with different data (S12) and an independent procedure (FFT) employed in the TSI forecast due to S13.

C. In Appendix B, based on both the Solar System movement reconstruction and simulation, H services, developed by the Solar System Dynamics Group of the JPL/NASA, and monthly SSN data from the World Data Center SILSO for the last decades, we have provided additional elements to support the idea that long-term solar activity is modulated by recurrent planetary effects. Our analysis establishes the following:

a) Solar System dynamics generate lateral forces (enhanced by its double integral) with multi-millennia scale (~9500 yr) oscillations similar to those shown by solar activity (enhanced by its double integral);

b) There is a suggested lagged response of around 67 centuries, of solar activity (enhanced by its double integral) to the gravitational forcing (lateral force). The maximum forces F precede the maximum solar activity TSI, meaning that increases (decreases) of force F produce lagged increases (decreases) of TSI;

c) Taking into account that the Sun's rotation axis is tilted by about 7.25 degrees from the axis of the Earth's orbit, the PGF are able to generate meridional forces and consequently meridional circulations in the Sun;

d) The lagged response appears to increase with forcing periods with a non-linear logarithmic function that implies temporal scale influences and possible connections with meridional circulations in different deep layers of the Sun;

e) The similarity of the ~9500yr TSI with the average SSN 10.5yr cycle, with scales differing at almost three orders of magnitude, suggests a self-similar process with a mechanism possibly linked to recurrent PGF in different scales.

D. The qualitative verification of the total solar irradiance (TSI) ~9.5Ky recurrent patterns with a bivalve population (BVp) reconstructed from late Miocene (~10.5Mya) data, shown in Appendix A, confirms not only the existence of this recurrent solar pattern throughout geological eras but also its persistent characteristics, period and pattern, because the comparison is made with the extrapolated forward in time TSI record (see Appendix A and Fig. 4).

Our experimental multi-millennial-scale analogue forecast of TSI, supported mainly by recurrent oscillations over the last glacial-interglacial cycle, shows a lowering trend toward a minimum for the coming decades. Our forecast also confirms previous efforts by several authors (Fairbridge and Sanders, 1987; Fairbridge and Shirley, 1987; Perry and Hsu, 2000; Duhau and Jager, 2010), who have forecasted a solar Grand Minimum for the upcoming decades. For instance, recent findings linked to periodicities of the solar tachocline and their physical interpretation may permit us to estimate that solar variability is presently entering into a long Grand Minimum, thus consisting of an episode of very low SA (Duhau and Jager, 2010).

Although the complete physical basis of this recurrent process is missing, there are several examples of physical and theoretical evidence that also support our findings. Firstly, it is important to highlight what Mackey (2007) has stated: “In several papers, Rhodes Fairbridge and co-authors described how the turning power of planets is strengthened or weakened by resonant effects between the planets, the sun and the sun´s rotation about its axis.”

Specifically, there are important works motivated by Rhodes Fairbridge and other researchers, providing a theoretical basis and practical evidences of resonant interactions, for instance:

A. Abreu et al. (2012) have shown the physical basis of a gravitational forcing of the solar tachocline variations. They developed a gravitational model for describing the time-dependent torque exerted by the planets on a non-spherical tachocline and compared the corresponding power spectrum with the reconstructed SA record. They find an excellent agreement between the long-term cycles in proxies of SA and the periodicities in the planetary torque (with a period from 50 to 504 yr).

B. Fairbridge and Sanders (1987) have indicated long-term variations due to planetary forcings. They follow Stacey (1963) who, based on the periodicities of planetary orbits, proposed a ~4.45 Kyr Outer Planets Restart (OPR) cycle. It is close to half of the ~9.5 Kyr detected periodic recurrence.

C. Looking for solar-planetary resonances of our detected ~9.5 Kyr, we compared the “biggest” solar system secular frequencies determined by Laskar et al., (2011) over 20 Ma for the four inner planets, and over 50 Ma for the five outer planets, corresponding to 45.184 and 49.880 Kyr, respectively. We found that the mean value of 47.532 Kyr is almost five times the solar period detected (47.532 Kyr = 5 x [9.56 Kyr]). This means that the solar inner and outer planets show a resonance (5:1) with the solar periodicity detected.

We have found and tested a recurrence of ~9500 yrs of SA that implies a solar Grand-minimum for the next one and a half centuries. However, we can also support our findings with other studies. For instance, the existence of different solar modes of activity (Grand minima, Regular, and a possible Grand maxima), which have also shown important temporal variations with asymmetries (Grand maxima significantly less often experienced than Grand minima) during the Holocene (Usoskin et al., 2014), would be considered expressions of our detected recurrent pattern of ~9500yrs.

In this work, we have forecasted a continuation of the solar decline for the next decades, which is supported through precursory signals during recent decades:

a) A steady and systematic decline in solar polar magnetic fields, starting from around 1995, which is well correlated with changes in meridional-flow speeds (Janardhan P., Bisoi, S. K., Gosain S., 2010)

b) A decline in solar wind micro-turbulence levels. Based on extensive interplanetary scintillation (IPS) observations at 327 MHz, obtained between 1983 and 2009, a steady and significant drop in the turbulence levels in the entire inner heliosphere, starting from around ~1995, was detected (Janardhan et al., 2011).

c) A significant reduced ionospheric cut-off frequency to radio waves, normally about 30 MHz, to well below 10 MHz (Janardhan et al., 2015a).

Also, in this work, we have forecasted a Grand solar-minimum, with sustained low solar activity for the next two centuries, which has been supported through a number of recent studies and their findings:

a) The continuation of this decline in solar activity is estimated to continue until at least 2020, and there is a good possibility of the onset of a Grand solar minimum from solar-cycle 26 onwards (2031) (Janardhan et al., 2015b).

b) Based on the S04 SA record, it has been shown that gradual (abrupt) changes in solar surface meridional flow velocity lead to a gradual (abrupt) onset of grand minima, and that one or two solar cycles before the onset of grand minima, the cycle period tends to become longer (Choudhuri and Karak, 2012; Karak and Choudhuri. 2011). It is noteworthy that surface meridional flows over Cycle 23

(Hathaway and Rightmire, 2010) have shown gradual variations, and Cycle 24 started 1.3 years later than expected.

5 Conclusions

An analysis and test of recurrent solar variability for the last millennia has been presented in this study. It was based on multi-millennia solar-related reconstructed records from different and valuable proxy information.

The tested existence of the ~9.5 Kyr period recurrent pattern suggests that SA is characterized by solar dynamics with long-term patterns. Considering that it has been suggested that the modulating oscillations of SA, around 84, 178 and 2400 years, are possibly related to the Sun's rotation rate and impulses of the torque in the Sun's irregular motion (Landscheidt, 1999; Fairbridge and Sanders, 1987; Charvátová, 1995; Charvátová, 2000), our results also suggest that similar mechanisms on the solar dynamo must be proposed for solar oscillations of around 9.5 Kyrs. This hypothesis should be tested, taking into account the results presented in this paper.

In this direction, we analyze two key evidences of the solar recurrent pattern. In Appendix A, we present a qualitative verification of the total solar irradiance (TSI) ~9.5Ky recurrent patterns with a bivalve population (BVp) reconstructed from late Miocene (~10.5Mya) data that shows the geological-scale persistence and regularities of the SA patterns, which can only be explained by a planetary gravitational forcing (PGF).

In Appendix B, we present an empirical analysis of solar PGF forcing due to lateral forces. We found that lateral forces generate a low-frequency (~9500 yr) signal that presents similarity with, and precedes by ~6700 yrs, low-frequency solar activity. This lag appears to be part of the non-linear lagged responses of solar activity to different time-lengths of PGF. We suppose that this lateral forcing could enhance the oblateness of the solar body, and tidal influences, and consequently, as Abreu et al. (2012) have also suggested, regular cycles of solar activity. Finally, we also find that the solar patterns of 9600 and 10.5 yrs are similar, suggesting a common gravitational origin.

With all of these recurrent and persistent phenomena, we have presented, tested and verified an experimental multi-millennial forecast technique for SA. We have provided elements and supporting recent studies on precursor signals of an entering into a Grand minimum SA mode.

The extreme duration of the last solar minimum is important evidence of longer cycles, similar to those presented before the start of the Maunder and Spörer minima.

We can conclude that the evidence provided is sufficient to justify a complete updating and reviewing of present climate models to better consider these detected natural recurrences and lags in solar processes.

Appendix A: Qualitative verification of total solar irradiance (TSI) ~9.5Ky recurrent patterns with a bivalve population (BVp) reconstructed from late Miocene (~10.5Mya) data

In a recent paper Harzhauser et al. (2013; H13 hereafter) analyze the explosive demographic expansion by dreissenid bivalves as a possible result of astronomical forcing. These authors: a) reconstruct the extinct bivalve species Sinucongeria primiformis in a lacustrine system of Lake Pannon during the Tortonian (~10.5 Mya; late Miocene), with 600 samples that cover about eight millennia of late Miocene time with a decadal resolution; and b) detect bivalve population regular fluctuations possibly linked to solar activity. H13 have pointed out: "Our data indicate that the settlement by bivalves in the off-shore environment was limited mainly by bottom water oxygenation, which follows predictable and repetitive patterns through time. These population fluctuations might be related to solar cycles: successful dreissenid settlement is recurring in a frequency known as the lower and upper Gleissberg cycles with 50–80 and 90–120 yr periods. These cycles appear to control regional wind patterns, which are directly linked to water mixing of the lake. This is modulated by the even more prominent 500 yr cycle, which seems to be the most important pacemaker for Lake Pannon hydrology."

In this Appendix A, we extend the H13 detected solar-terrestrial connections (TSI-BVp) to the complete reconstructed ~8Kyr BVp record, comparing the reconstructed record with the average of the S04, S09 and S12 TSI records extrapolated forward in time (Fig 4.).

An initial comparison, shown in Figure A.1, demonstrates the existence of millennia and multi-millennia scale oscillation in TSI and BVp series of anomalies. However, when an adjustment (a linear transformation) and a lower threshold for TSI are applied, the following comparison, shown in Figure A.2, better demonstrates the existence of millennia and multi-millennia-scale similar oscillation in TSI and BVp series of anomalies.

This simple trend adjustment of the TSI could be justified by the orbital phenomena of eccentricity and obliquity that can modulate solar influences in periods of 100 and 40 Kyr, respectively. Additional adjustments in the BVp timing could improve the match.

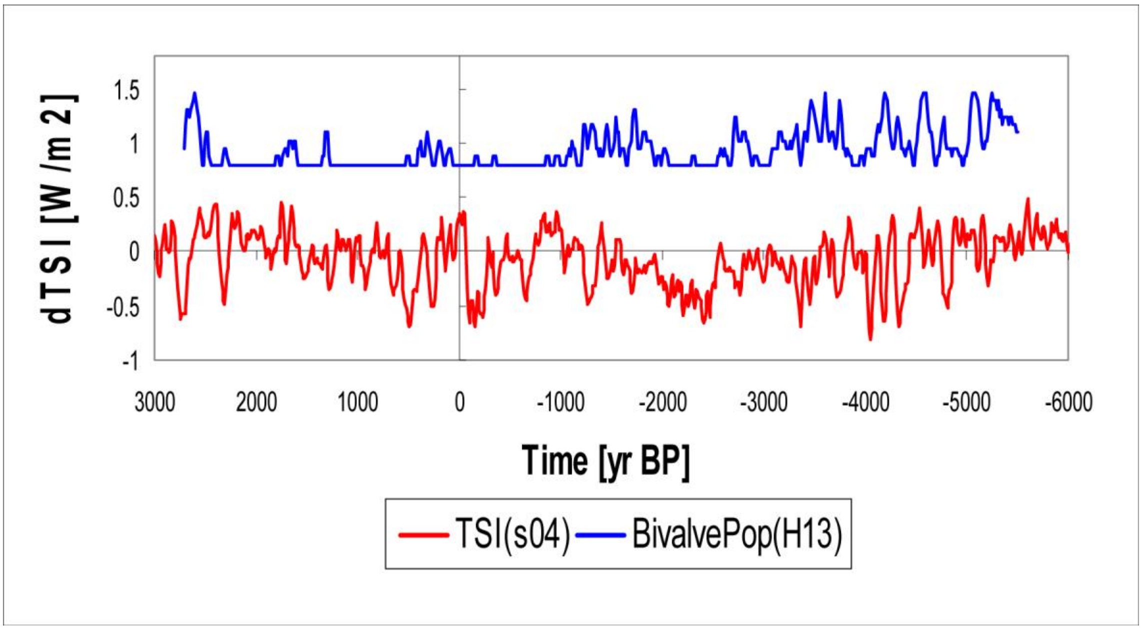

Figure A.1. Comparison of bivalve population (BVp) and TSI. A linear transformation [BVp(H13) = aBVp(H13) + b] with a factor a=0.22 and a bias b=0.8.

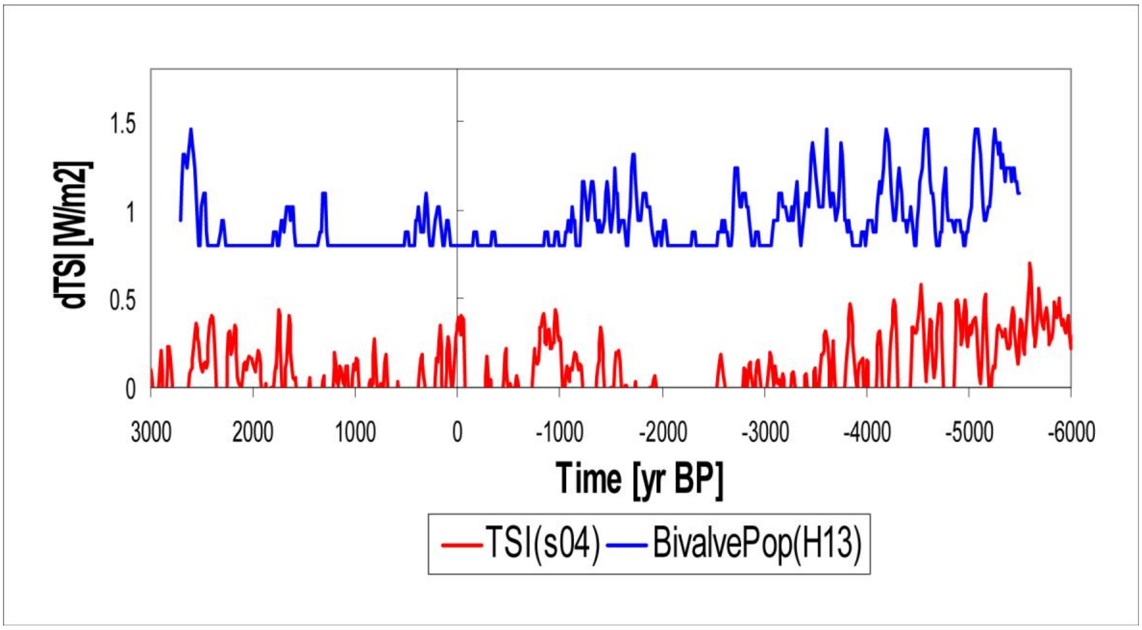

Figure A.2. Comparison of bivalve population (BVp) and TSI adjusted with a linear transformation [TSIadj=TSI+a(t-t1)+b] with a=.03 [W/m2]/1000[yr] and b=-0.3 [W/m2]. Only positive TSI adjusted anomalies are displayed in order to enhance the match and show a possible threshold provided by TSI for BVp development.

Appendix B: Empirical evidence of a lagged planetary gravitational forcing of the ~9500yr total solar irradiance (TSI) recurrent pattern

Planetary gravitational forcing (PGF) of solar activity (SA) has been considered by many solar researchers (see references in the main part). However, numerical simulations of this forcing have been analyzed by only a few of them. For instance, Abreu et al. (2012) analyzed the PGF of solar tides. In this Appendix, we compare the lateral (perpendicular to movement) forces evaluated by lateral accelerations of the solar movement around the solar system (SS) barycenter (BC) with TSI reconstructed and extrapolated (based on the detected recurrences) records. Our work is motivated by the findings from Fairbridge and Shirley (1987), who predicted the initiation of a Maunder-type prolonged solar minimum on the basis of a study of solar motion with respect to the SS-BC in the years from 760 to 2100 AD. Their study detected "patterns" in solar orbits associated with different levels of SA.

In order to analyze variability in both solar dynamics and solar activity, we studied data coming from: a) lateral forces (F) of the sun due to planetary gravitational forces and movements, reconstructed and forecasted by JPL/NASA from 3000 BC to 3000 AD, and b) solar activity expressed in the total solar irradiance (TSI) average from three reconstructed records over the last millennia and extrapolated for the next millennia (all shown in Figures 4a). These two records are displayed in Figure B.1.

Lateral (perpendicular to movement) forces were evaluated based on X, Y and Z coordinates and derivatives provided by the HORIZONS (H) system from the Jet Propulsion Laboratory/NASA (JPL/NASA) for the past 5000 and future 1000 years, every 90 days, where the XY plane is the ecliptic plane centered on the BC. As an approximation, solar movement was considered only in the XY plane, and lateral acceleration in this plane was evaluated to be perpendicular to the tangential direction of solar movement. These on-line solar system data and ephemeris computation services provide accurate ephemerides for solar system objects.

The simulated lateral inertial forces (F) are considered to provide gravitational influences on solar activity. In order to enhance their low-frequency oscillations, we applied the double integral function to the analyzed F record.

An integration was applied twice to the Solar signal, *S(t)*, as follows:

$$\sigma S_1(t) = \int_{t_0}^{t} (S\ (t) - \mu_S)\,dt \qquad \text{(B1)}$$

$$\sigma S_2(t) = \int_{t_0}^{t} (\sigma S_1(t) - \mu_{S1})\,dt \qquad \text{(B2)}$$

Where, *S(t)* is the solar signal, expressed as force (*F(t)*) or **as** total irradiance (*T(t)*), *t* is time, t_0 is initial time, $\sigma S_N(t)$ is its time integral, N is the successive application number, and μ_S and μ_{S1} are the long-term averages of *S(t)* and $\sigma S_1(t)$, respectively.

We apply equations B1 and B2 to these two records in order to enhance low-frequency variations. Results are displayed in Figure B.2. The double integral of forces $F, \sigma F_2(t)$, is almost explained (99.9 % of variance) by a sine function of a 9400 yr oscillation, which is also displayed in Fig. B.2a. The double integrated solar activity TSI, $\sigma T_2(t)$, also shows a periodicity of ~9500 yrs. The scales of these enhanced solar signals are inverted because the sign is changed due to the double integration enhancement. A comparison of both curves is displayed in Figure B.3a. Figure B.3b also displays both integrated curves, however the $\sigma T_2(t)$ curve is leaded (moved backward in time) 6700 yrs.

In order to verify this 6700 yr lag of the TSI response to the F oscillation of a 9500 yr period, we look for two other similar pairs of periods and lags (P/L). In order to obtain an additional pair of P/L, we analyze the lateral force F and solar activity TSI over the 1000-3000 AD period. We applied a double integration (Eq. B1) and a polynomial detrending process to F. The $\sigma T_2(t)$ and its trend is shown in Figure B.4. The detrended $\sigma T_2(t)$ is compared with the TSI record, and oscillations of ~950 yrs are detected, together with a lag of ~350 yrs of TSI with respect to the supposed forcing F. These two variables are displayed in Figure B.5.

Another pair of P/L values is evaluated with the Hale SSN cycle of ~22 years that shows an alternating magnetic sign for each 22 yrs. It is compared with the Fourier series (with only 2 harmonics) of the force F, signal based on the period from 1700 to 2000 AD. The comparison, depicted in Figure B.6, indicates a lag of less than 1 year.

The three sets of L/P pairs are 1/22, 350/950 and 6700/9500 yrs, respectively. These three pairs, which correspond to different phases, are modeled together with a non-linear function that tends toward a lower limit of 0° for lower periods, and an upper asymptotic limit of 360°

(2*Pi radians). The adjusted model for phase variations in terms of period, which is a logarithmic function, is depicted in Figure B.7.

It is important to emphasize that the results in Figure B.5 have not only detected an L/P pair but also confirm the next forecasted Grand Minima (2020-2220 AD) also associated with contributions from unexplained modulation process of ~350-yr-lagged-influences of solar lateral forces.

Additionally, we developed an interesting comparison that shows self-similarity in TSI. This comparison is for our enhanced $\sigma T_2(t)$ ~9500yr-solar-cycle, evaluated previously, with a Fourier series model of the solar SSN cycle with a period of 10.5yrs, based on monthly SSN data from the World Data Center SILSO, Royal Observatory of Belgium, Brussels, over the period from 1964 to 2008. This comparison is displayed in Figure B.8, and clearly shows self-similarities between these two solar cycles. Both cycles show a shorter increasing period (~25%) than the decreasing period (~45%), and a maximum plateau (~20%), and an almost nonexistent minimum plateau.

Finally, we also developed a spectral analysis of the analyzed lateral forces. This analysis is based on wavelets and is displayed in Figure B.9. It clearly shows important contributions to periods around of 12, 22, 60 (in a range of 50-80), 180, 650 (in a range of 400-800), 1000 and 2600 years.

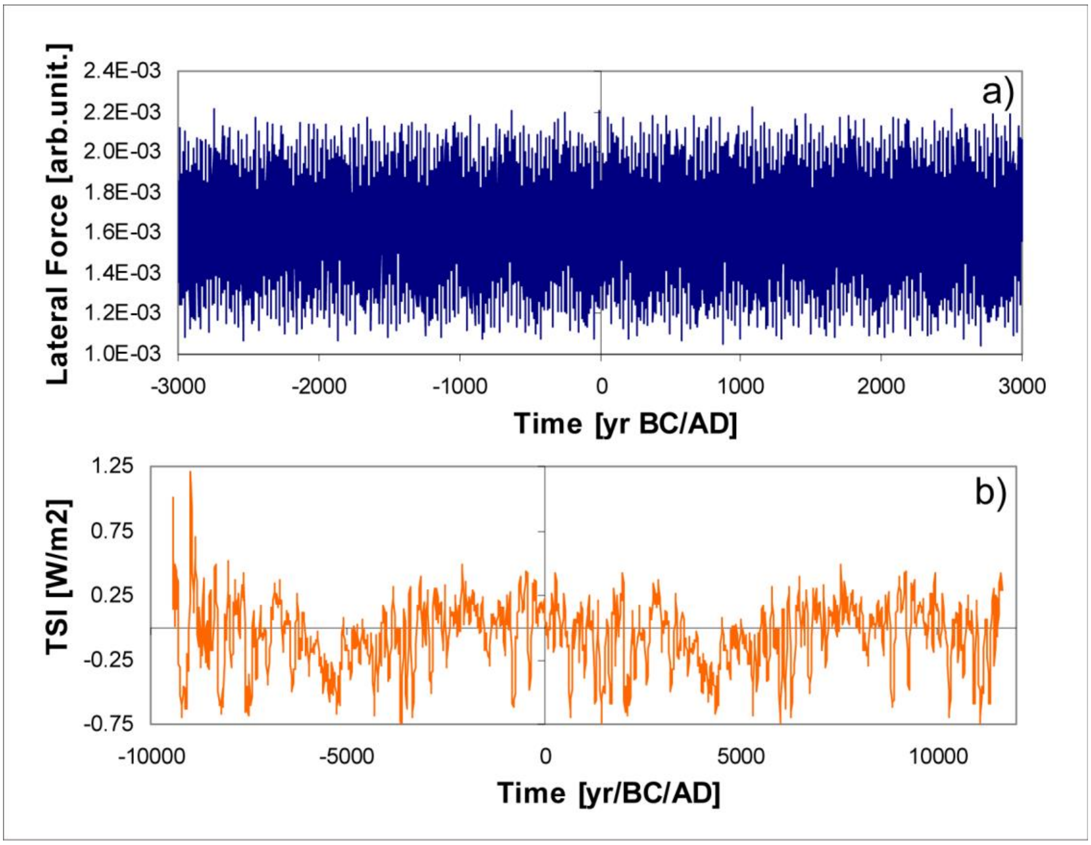

Figure B.1. a) Lateral forces on the Sun generated by planetary gravitational forces (PGF), expressed in [arbitrary units], evaluated by the Horizon/NASA system from 3000 BC to 3000 AD. b) The solar activity (TSI) expressed in [W/m2], average values of the three reconstructed records over the last millennia and extrapolated for the next millennia (10000 BC to 10000 AD) based on ~9500 yr recurrence (records shown in Figure 3a).

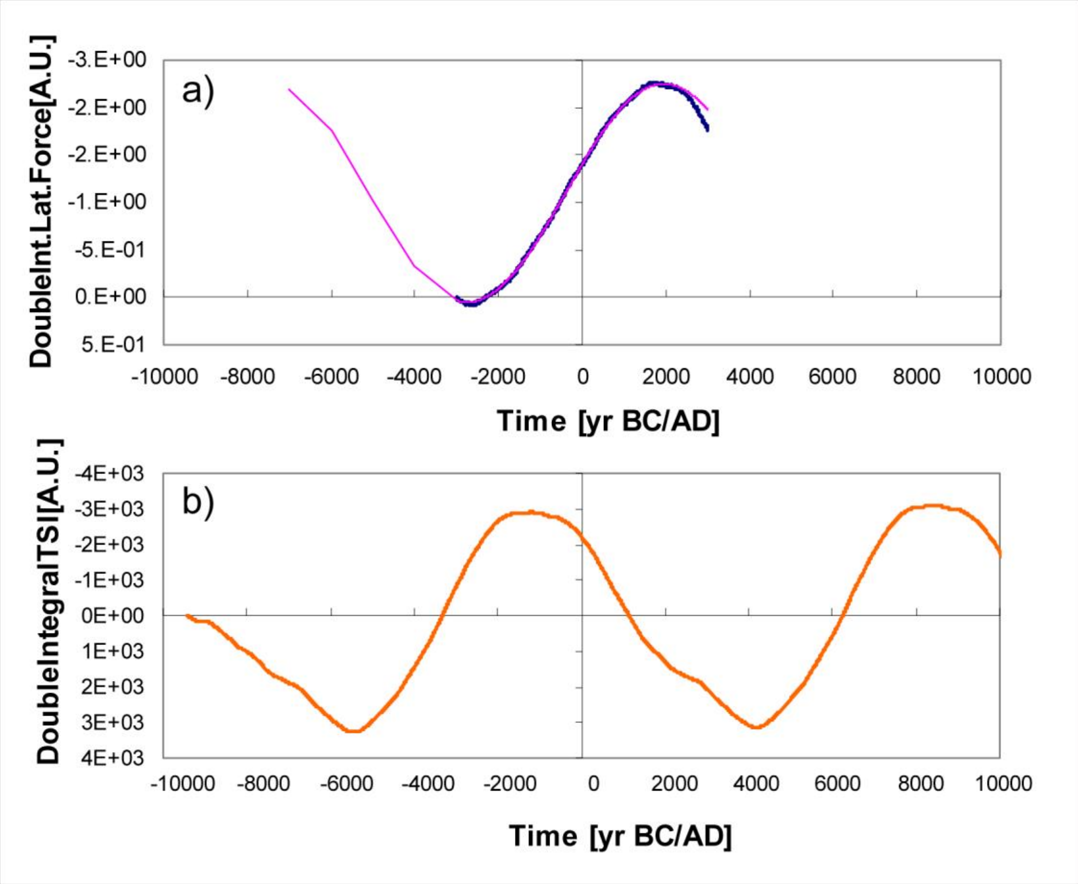

Figure B.2. a) Double integral of the solar lateral inertial forces $\sigma F_2(t)$ due to the solar movement resulting from the planetary gravitational forces shown in Figure B.1.A, and b) Double integral of the solar reconstructed and extrapolated record $\sigma T_2(t)$ shown in Figure B.1.B. Vertical scale of values were inverted both in $\sigma F_2(t)$ and $\sigma T_2(t)$ because the double integral procedure changes the sign of the enhanced result. Please note that the last minimum of lateral inertial force F was around 2500 BC and the next minimum of TSI will be expected around 4200 AD. Please note the time difference between these minima of around 6700 yrs.

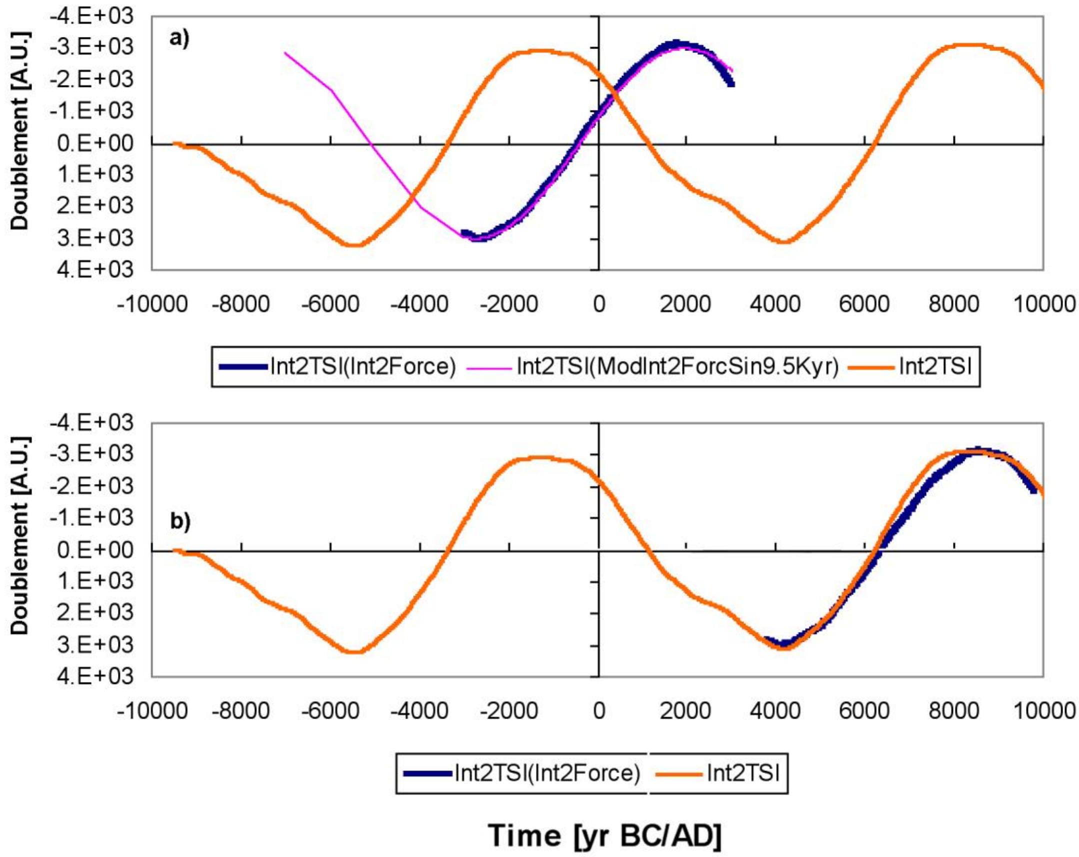

Figure B.3. A comparison of the double integral of the Double integral of the solar reconstructed and extrapolated record $\sigma T_2(t)$ and the model based on solar lateral inertial forces $\sigma F_2(t)$, $\sigma T_2(t)$ [$\sigma F_2(t)$]. To enhance a possible cause-effect relationship [$\sigma F_2(t)$ - $\sigma T_2(t)$] the $\sigma T_2(t)$ [$\sigma F_2(t)$] record is shown a) without and b) with a lag of 6700yrs. Vertical scale of values were inverted because the double integral procedure changes the sign of the enhanced result, thus upper/lower values indicate maxima/minima.

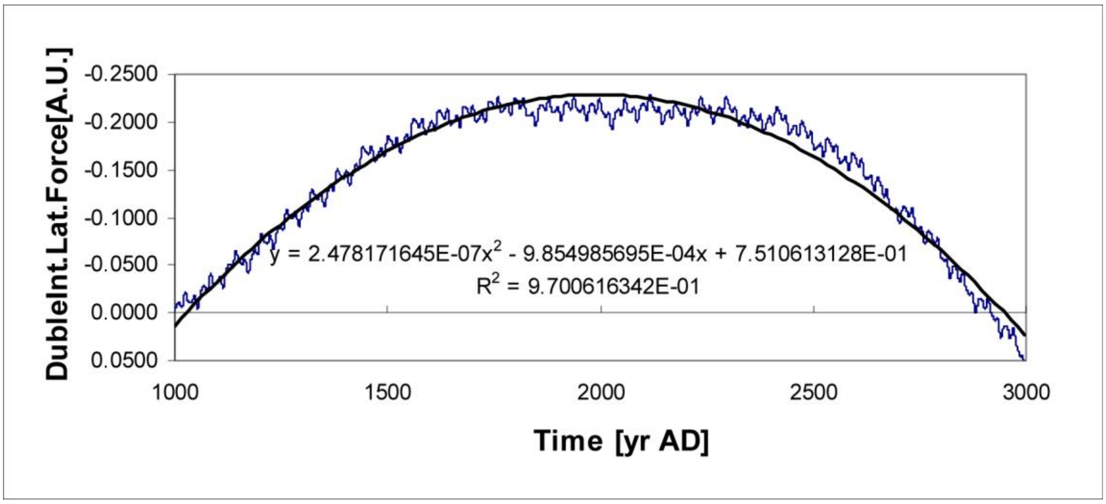

Figure B.4. The double integral of the solar lateral inertial forces $\sigma F_2(t)$ for the period from 1000 to 3000 AD. A polynomial trend is also depicted.

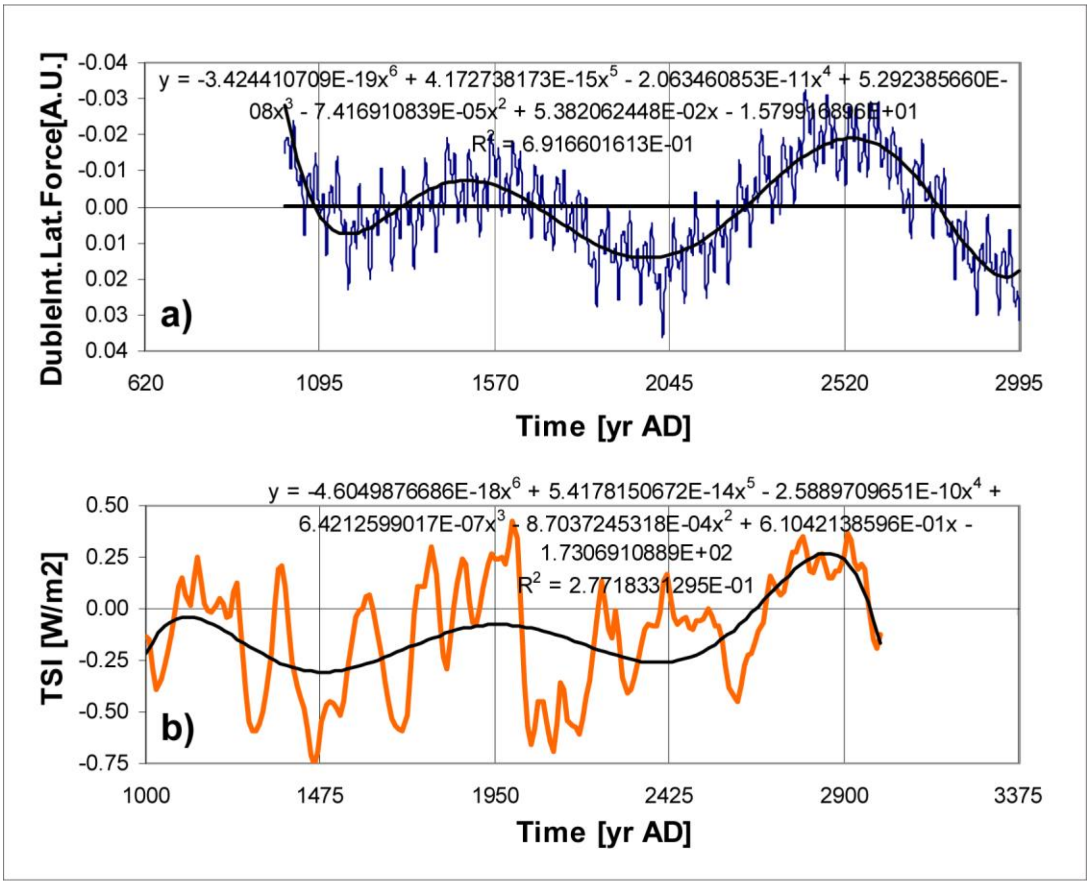

Figure B.5. A comparison of the double integral of the solar lateral inertial forces $\sigma F_2(t)$ and the solar reconstructed and extrapolated record TSI. To enhance trends, polynomials are adjusted to both records, showing oscillations of ~950 yrs and a lag of ~350 yrs.

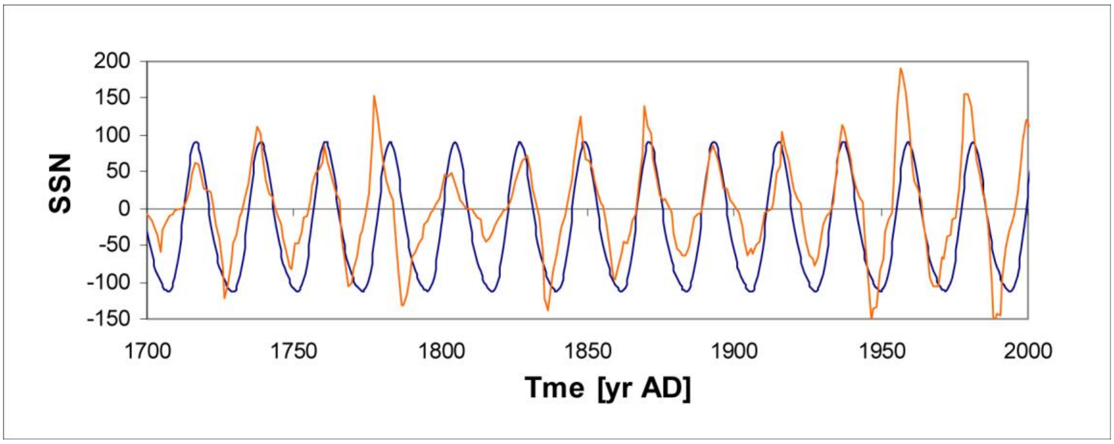

Figure B.6. A comparison of the Hale solar cycle of SSN and the Fourier Series (with only 2 harmonics) model of the F signal. A lead of 0.5 yrs is applied to the SSN to improve the match with the F recurrent model.

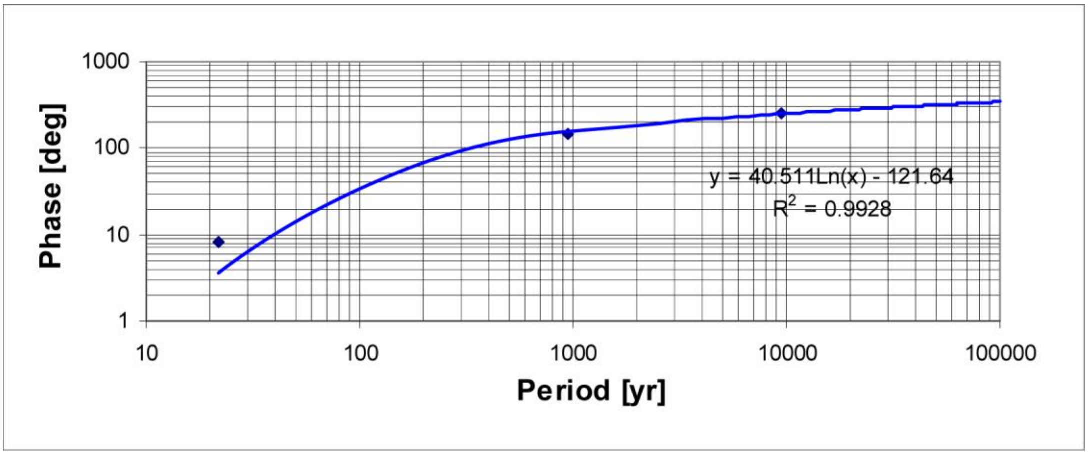

Figure B.7. A model of phase between F (forcing) and TSI (suggested response) signals for different periods. The adjusted logarithmic model, which explains 99.5 % of the variance, shows two trends, one to zero for short periods, and other, an asymptotic one, for long periods.

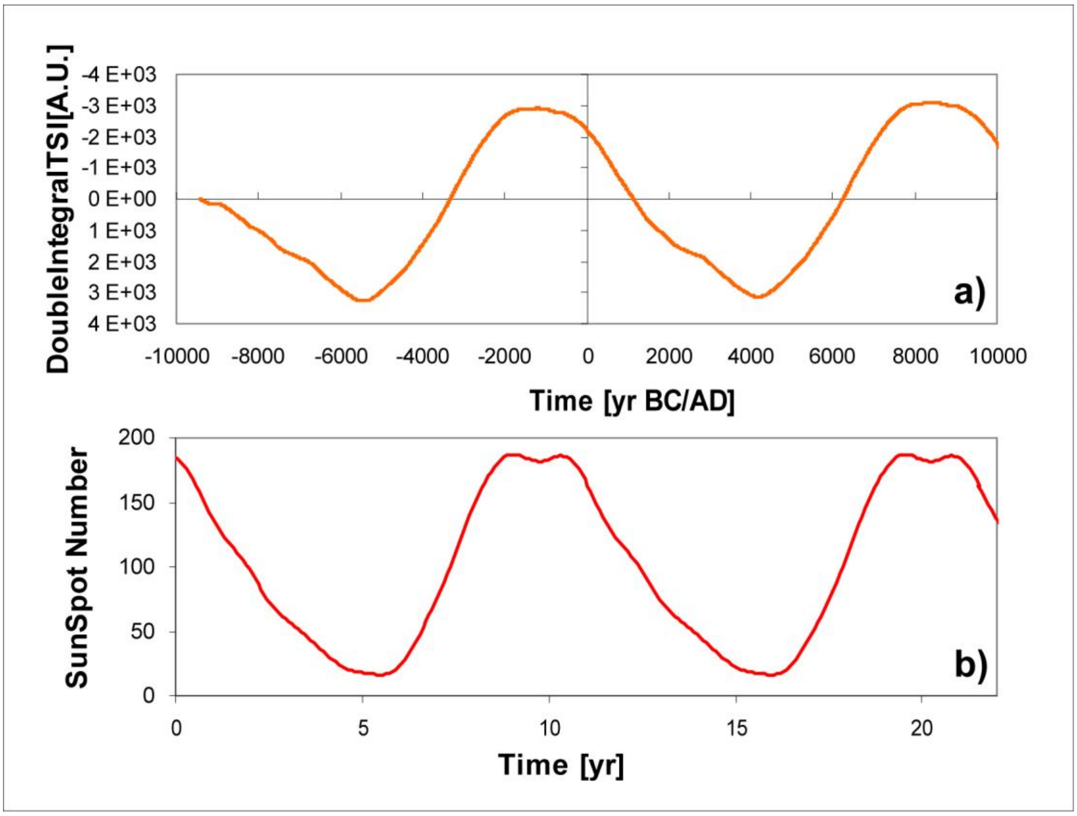

Figure B.8. Comparison of: a) the double integral of the reconstructed solar activity (TSI) [Vertical scale of values were inverted because the double integral procedure changes the sign of the enhanced result], and b) the mean solar cycle obtained with a FS model based on SSN data from the World Data Center SILSO, Royal Observatory of Belgium, Brussels, over the period from 1964 to 2008.

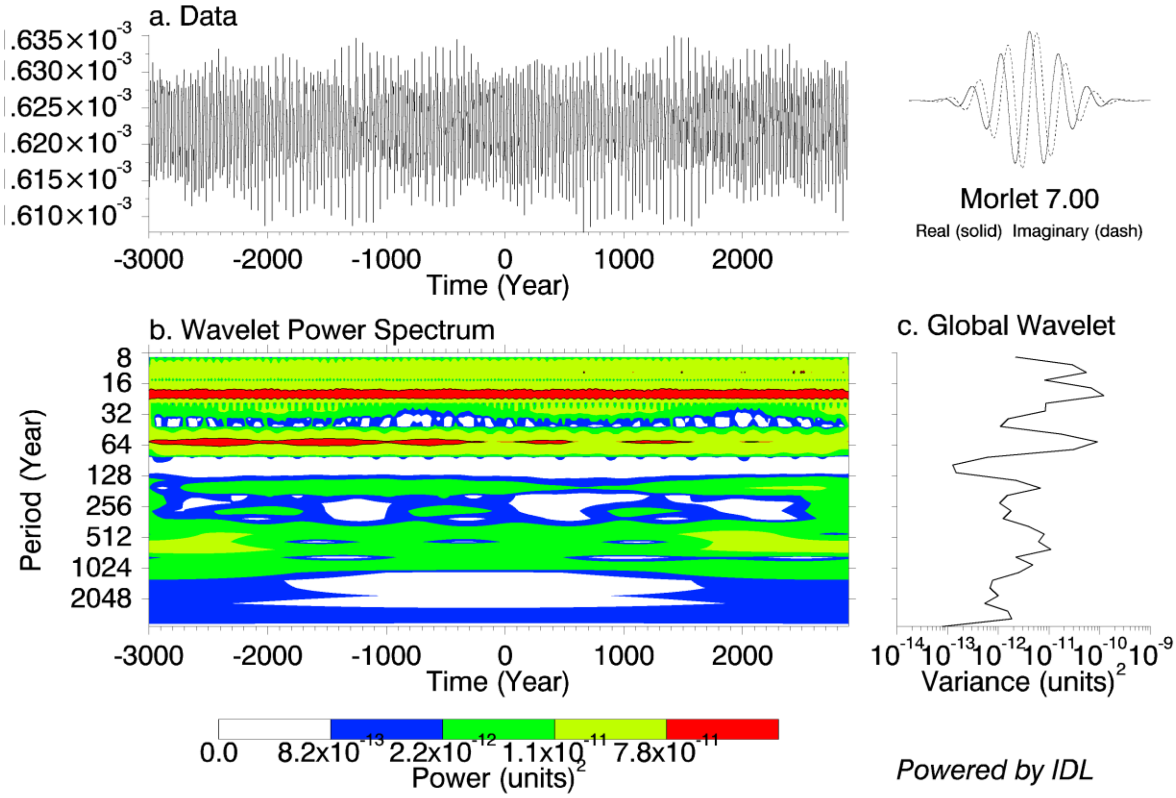

Figure B.9. (a) Lateral Force [arbitray units]. (b) The wavelet power spectrum. The contour levels are chosen so that 75%, 50%, 25%, and 5% of the wavelet power is above each level, respectively. The cross-hatched region is the cone of influence, where zero padding has reduced the variance. (c) The global wavelet power spectrum (black line). The dashed line is the significance for the global wavelet spectrum, assuming the same significance level and background spectrum as in (b). Reference: Torrence, C. and G. P. Compo, 1998: A Practical Guide to Wavelet Analysis. Bull. Amer. Meteor. Soc., 79, 61-78.

Acknowledgements

This work was motivated by Rhodes Fairbridge's work around the idea that the solar system regulates the solar and Earth's climate (Mackey, 2006). The author thanks Professor Jan Veizer for his encouraging comments. The author also thanks Jana Schroeder, for her editorial contributions, and Oscar Alonso and Ricardo Espinoza, for their graphical contributions to this work. This work was initiated when the author was supported (2008-2012) by a NSF grant (GEO-0452325) through the IAI project CRN-II-2050 and by Institute UC MEXUS and CONACYT through an international collaborative project between IMTA and SIO/UCSD under the 2008 Climate Change Program.

References

Abreu J.A., C. Albert, J. Beer, A. Ferriz-Mas., K. G. McCracken, and F. Steinhilber (2012), Is there a planetary influence on solar activity? *Astronomy and Astrophysics*, 548, A88.

Adolphi, F., Muscheler, R., Svensson, A., Aldahan, A., Possnert, G., Beer, J., Sjolte, J., Björck, S., Matthes, K., and Thiéblemont, R. (2014), Persistent link between solar activity and Greenland climate during the Last Glacial Maximum, Nat. Geosci., 7, 662–666, doi: 10.1038/ngeo2225, 2014.

Charvátová, I. (1995), Solar-terrestrial and climatic variability during the last several millennia in relation to solar inertial motion, J. Coastal Res., 17, 343-354.

Charvátová, I. (2000), Can origin of the 2400-year cycle of solar activity be caused by solar inertial motion? Ann. Geophys., 18, 399-405.

Choudhuri, A.R. and Karak, B.B. 2012. The origin of grand minima in the sunspot cycle, Phys.Rev. Lett., 109,171103.

Cuffey, K. M., and G. D. Clow (1997), Temperature, accumulation, and ice sheet elevation in central Greenland through the last deglacial transition, Journal of Geophysical Research, 102:26383-26396.

Duhau, S. and C. de Jager (2010), The Forthcoming Grand Minimum of Solar Activity, Journal of Cosmology, 8, 1983-1999.

Eddy, J. A. (1981), Climate and the Role of the Sun, in Climate and History, (R. I. Rotberg and T. K. Rabb, Eds.) Princeton University Press, Princeton, New Jersey, 145-168.

Fairbridge, R. W., and J. E. Sanders (1987), The Sun's orbit AD 750-2050. Basis for new perspectives on planetary dynamics and Earth-Moon linkage, in: Rampino, M. R., J. E. Sanders, W. S. Newman, and L. K. Königsson, (eds.), Climate, history and predictability, Van Nostrand-Reinhold, New York, 446-471.

Fairbridge, R. W., and J. H. Shirley (1987), Prolonged minima and the 179-yr cycle of the solar inertial motion, Sol. Phys., 110, 191-220.

Finkel, R. C., and K. Nishiizumi (1997), Beryllium 10 concentrations in the Greenland Ice Sheet Project 2 ice core from 3-40 ka, Journal of Geophysical Research, 102:26699-26706.

Harzhauser, M., Mandic, O., Kern, A.K., Piller, W.E., Neubauer, T.A., Albrecht, C., Wilke, T. 2013. Explosive demographic expansion by dreissenid bivalves as a possible result of astronomical forcing. Biogeosciences, 10, 8423-8431.

Hathaway D.H. and Rightmire, L. 2010. Variations in the Sun's Meridional Flow over a Solar Cycle, Science, Vol. 327, No. 5971, pp. 1350-1352, doi: 10.1126/science.1181990.

HORIZONS System. Documentation of JPL Horizons (Version 3.75) Apr 04, 2013. ftp://ssd.jpl.nasa.gov/pub/ssd/Horizons_doc.pdf. [Data retrieved at: www.ssd.jpl.nasa.gov/?horizons]

Janardhan P., Bisoi, S.K., Gosain S. 2010. Solar Polar Fields During Cycles 21 – 23: Correlation with Meridional Flows, Solar Physics, December 2010, Volume 267, Issue 2, pp 267-277, doi: 10.1007/s11207-010-9653-x.

Janardhan, P., Bisoi, S.K., Ananthakrishnan, S., Tokumaru, M., and Fujiki, K. 2011. The prelude to the deep minimum between solar cycles 23 and 24: Interplanetary scintillation signatures in the inner heliosphere, Geophys. Res. Lett., 38, L20108, doi: 10.1029/2011GL049227.

Janardhan, P., Bisoi S.B., Ananthakrishnan, S., Tokumaru, M., Fujiki, K., Jose, L., and Sridharan, R. 2015. A 20 year decline in solar photospheric magnetic fields: Inner-heliospheric signatures and possible implications, J. Geophys. Res.: Space Physics, 120(7), 5306–5317, doi: 10.1002/2015JA021123.

Janardhan, P., Bisoi S.B., Ananthakrishnan, S., Sridharan, R., and Jose, L. 2015. Solar and Interplanetary Signatures of a Maunder-like Grand Solar Minimum around the Corner - Implications to Near-Earth Space, Sun and Geosphere, Special Issue: UN/Japan Workshop on Space Weather. Sun and Geosphere, Vol 10, No. 2, 147-156, 2015.

Jose, P. D. (1965), Sun's Motion and Sunspots, Astron. J., 10(1), 193-200.

Karak, B.B. and Choudhuri, A.R. 2011. Is meridional circulation important in modelling irregularities of the solar cycle? Comparative Magnetic Minima: characterizing quiet times in the Sun and stars. Proceedings IAU Symposium No. 286, 2011, A.C. Editor, B.D. Editor & C.E. Editor, eds. International Astronomical Union.

Keeling, C. D., and T. P. Whorf, (2000), The 1,800-year oceanic tidal cycle: A possible cause of rapid climate change, Proc. Natl. Acad. Sci. U. S. A., 97 (8), 3814–3819.

Kindler, P., Guillevic, M., Baumgartner, M., Schwander, J., Landais, A., and Leuenberger, M.: Temperature reconstruction from 10 to 120 kyr b2k from the NGRIP ice core, Clim. Past, 10, 887-902, doi: 10.5194/cp-10-887-2014, 2014.

Landscheidt, T. (1999), Extrema in sunspot cycle linked to Sun's motion, Sol. Phys., 189, 413-424.

Laskar, J., A. Fienga, M. Gastineau, and H. Manche (2011), La2010: A new orbital solution for the long-term motion of the Earth, Astronomy & Astrophysics, 532 (A889).

Mackey, R. (2007), Rhodes Fairbridge and the idea that the solar system regulates the Earth’s climate, Journal of Coastal Research, Special Issue 50 (Proceedings of the 9th International Coastal Symposium), 955 - 968. Gold Coast, Australia.

Muscheler, R., and U. Heikkilä (2011), Constraints on long-term changes in solar activity from the range of variability of cosmogenic radionuclide records, Astrophys. Space Sci. Trans., 7, 355-364, doi: 10.5194/astra-7-355.

Perry, C. A., and K. J. Hsu (2000), Geophysical, archaeological, and historical evidence support a solar-output model for climate change. Proceedings of the National Academy of Sciences USA, 97, 12,433-12,438.

Ruzmaikin, A. A. (1983), Nonlinear problems of the solar dynamo, in: Soward, A. M. (ed.): Stellar and Planetary Magnetism, Gordon Breach, New York, 151.

Schmitt, D., M. Schussler, and A. Ferriz-Mas (1996), Intermittent solar activity by an on-off dynamo, Astron. Astrophys., 311, L1.

Shaviv N. J., A. Prokoph, and J. Veizer (2014), Is the solar system's galactic motion imprinted in the Phanerozoic climate?, Sci Rep., Aug 21;4:6150. doi: 10.1038/srep06150.

Shirley, J. H., and R. W. Fairbridge (Eds.) (1997), Encyclopedia of Planetary Sciences, Chapmann & Hall.

SILSO, World Data Center - Sunspot Number and Long-term Solar Observations, Royal Observatory of Belgium, on-line Sunspot Number catalogue: [Data retrieved at: http://www.sidc.be/silso/datafiles].

Solanki, S. K., I. G. Usoskin, B. Kromer, M. Schüssler, and J. Beer (2004), Unusual activity of the Sun during recent decades compared to the previous 11,000 years, Nature, Vol. 431, No. 7012, 1084–1087.

Stacey, C. (1967), Earth motions and time and astronomic cycles. Pages 335-340 and 999-1003 in The Encyclopedia of Atmospheric Sciences and Astrogeology, R. Fairbridge, editor, Reinhold Publishing, New York.

Stacey, C. M. (1963), Cyclic measure. Some tidal measures concerning equinoctal years, Ann. New York Acad. Sciences, No. 6.

Steinhilber, F., J. Beer, and C. Frohlich (2009), Total solar irradiance during the Holocene, Geophysical Research Letters, 36, doi: 10.1029/2009GL040142.

Steinhilber, F., J. A. Abreu, J. Beer, I. Brunner, M. Christl, H. Fischer, U. Heikkilä, P. W. Kubik, M. Mann, K. G. McCracken, H. Miller, H. Miyahara, H. Oerter, and F. Wilhelms (2012), 9,400 years of cosmic radiation and solar activity from ice cores and tree rings, Proc. Natl. Acad. Sci. USA, 109. doi: 10.1073/pnas1118965109.

Steinhilber F., and J. Beer (2013), Prediction of solar activity for the next 500 years, J. Geophys. Res. Space Physics, 118, doi:10.1002/jgra.50210.

Sturevik-Storm, A., Aldahan A., Possnert G., Berggren A.M., Muscheler R., Dahl-Jensen D., Vinther B.M., Usoskin I6. (2014), 10Be climate fingerprints during the Eemian in the NEEM ice core, Greenland, Nature/Sci.Rep., 4, 6408; DOI:10.1038/srep06408.

Torrence, C., and G. P. Compo (1998), A Practical Guide to Wavelet Analysis, B. Am. Meteorol. Soc., 79, 61-78.

Usoskin, I.G., Hulot, G., Gallet, Y., Roth, R., Licht, A., Joos, F., Kovaltsov, G.A., Thebault, E. and Khokhlov, A. 2014. Evidence for distinct modes of solar activity. Astronomy and Astrophysics 562: L10, DOI:10.1051/0004-6361/201423391.

Velasco Herrera, V. M., B. Mendoza, and G. Velasco Herrera (2015), Reconstruction and prediction of the total solar irradiance: From the Medieval Warm Period to the 21st century, New Astronomy, 34, 221, DOI: 10.1016/j.newast.2014.07.009

Vlahos, L., Georgoulis, M.K. (2004), On the Self-Similarity of Unstable Magnetic Discontinuities in Solar Active Regions. Astrophys. J. Lett. 603, L61–L64. doi:10.1086/383032

Xapsos, M., and E. Burke (2009), Evidence of 6000-year periodicity in reconstructed sunspot numbers, Sol. Phys., 257 (2), 363-369.

Figure Legends

Figure 1. Solar-related and climate signals. (a) Solar activity, TSI, reconstructed by S04, S09 and S12, after an intercalibration using the S09 record as a base. (b) 10Be isotope concentration in polar ice cores during the past 130 Kyrs (Finkel and Nishiizumi, 1997; FN97; Stuverik-Storm et al., 2014; SS14). (c) 10Be isotope concentration in Greenland ice cores during the period from 19 to 11 Kyr BP (Adolphi et al., 2014; A14). Please note that in all figures: as the 10Be concentration varies inversely with Solar activity, TSI, the beryllium scales are inverted, and thus the upper parts in these scales indicate high TSI levels.

Figure 2. Data and modelling of 10Be isotope concentration in Greenland ice cores. a) Data and a FS model of 10Be isotope for the past 40 Kyrs provided by (Finkel and Nishiizumi, 1997; FN97) after detrended and demodulated (See SI). b) The model, shown in a), is extrapolated covering the last 135 Kyrs, and the (Stuverik-Storm et al., 2014; SS14) data is included for comparison. c) A zoom of b) for a detailed comparison of the extrapolated FS model and the SS14 data. Please note that a maximum match implies a SS14 temporal adjustment, or time bias, of 1.5 Kyrs going back in time.

Figure 3. A test of the recurrent TSI signal based on 14C over the last 11000 yrs, TSI(S04), and the linear model based on the 10Be isotope concentration record from Greenland ice cores. We extrapolated the TSI(S04) record backward in time, 9400 yrs, to match the model based on 10Be isotope (A14) that covers the period from 18000 to 10000 yrs BP.

Figure 4. Solar activity signals reconstructed and modelled records. (a) Solar activity, TSI, reconstructed by Solanki et al. (2004), Steinhilber et al. (2009), and Steinhilber et al. (2012) (S04, S09 and S12, respectively), shown in Figure A, and their analogue models. (b) A zoom of a) that covers only 2Kyr. (c) Another greater zoom of a) that covers only 0.85Kyr including the independent TSI forecast by S13. (d) The CTC Tcrb signal and its simple model including the independent TSI forecast by S13. Big and small vertical arrows indicate Super and Grand solar minima.

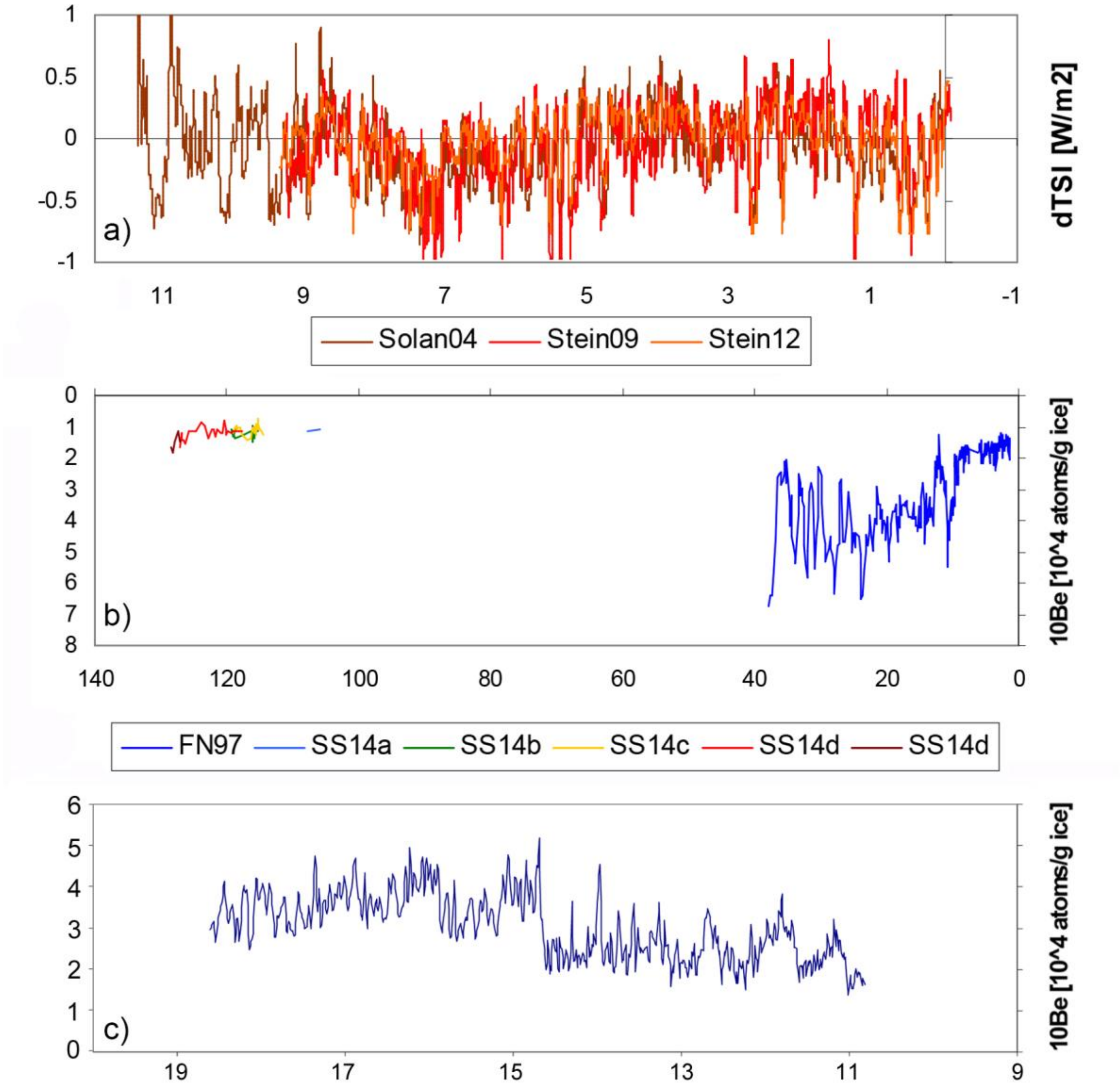
a)
dTSI [W/m2]
Solan04
Stein09
Stein12
b)
10Be [10^4 atoms/g ice]
FN97
SS14a
SS14b
SS14c
SS14d
SS14d
c)
10Be [10^4 atoms/g ice]

Figure 1.

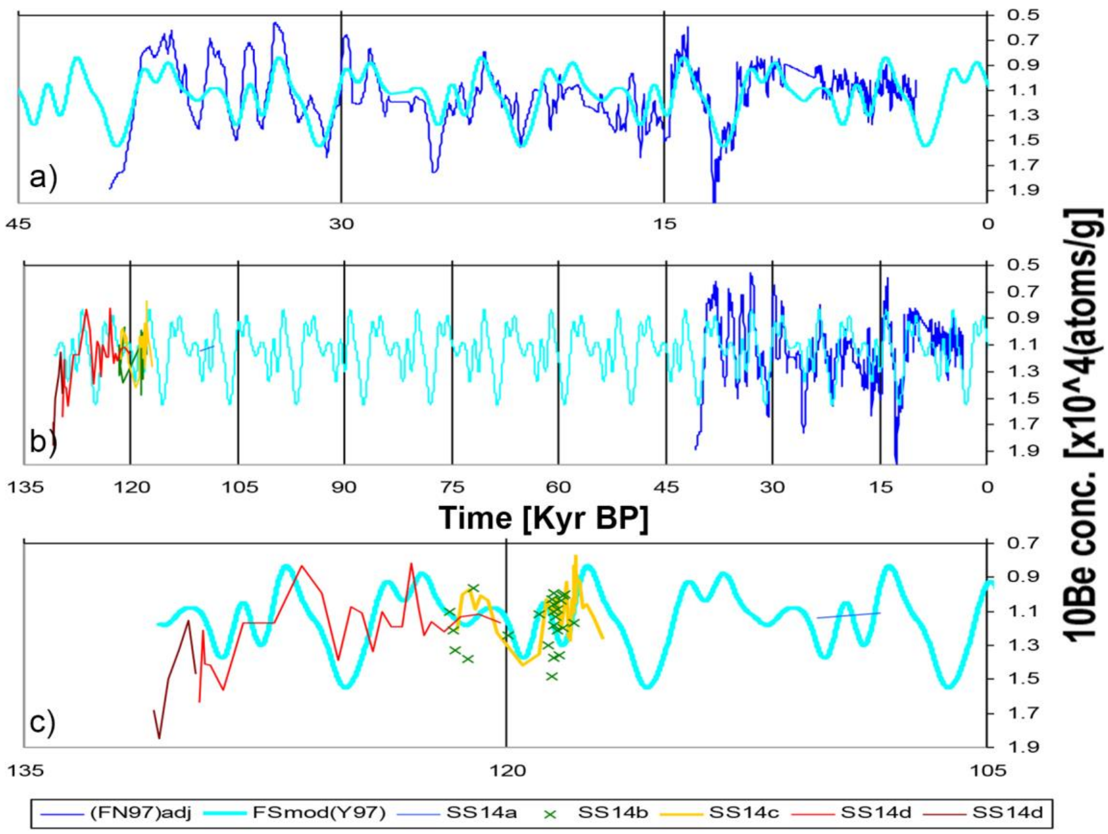

a)
b)
c)
45
30
15
0
135
120
105
90
75
60
45
30
15
0
Time [Kyr BP]
135
120
105
0.5
0.7
0.9
1.1
1.3
1.5
1.7
1.9
10Be conc. [x10^4(atoms/g)]
(FN97)adj
FSmod(Y97)
SS14a
SS14b
SS14c
SS14d
SS14d

Figure 2.

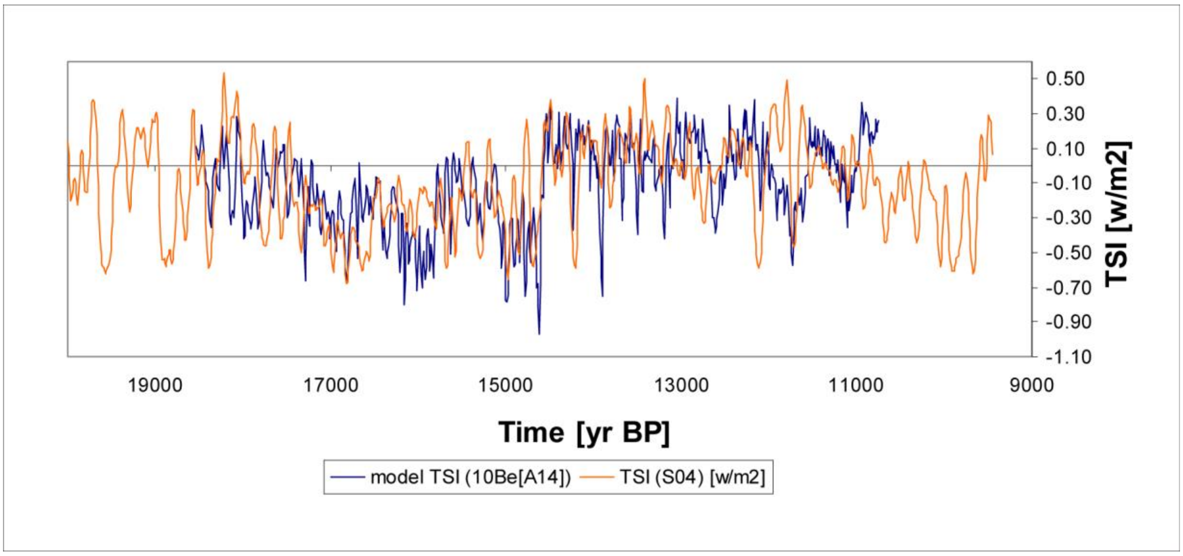
0.50
0.30
0.10
-0.10
-0.30
-0.50
-0.70
-0.90
-1.10
TSI [w/m2]
19000
17000
15000
13000
11000
9000
Time [yr BP]
model TSI (10Be[A14])
TSI (S04) [w/m2]

Figure 3.

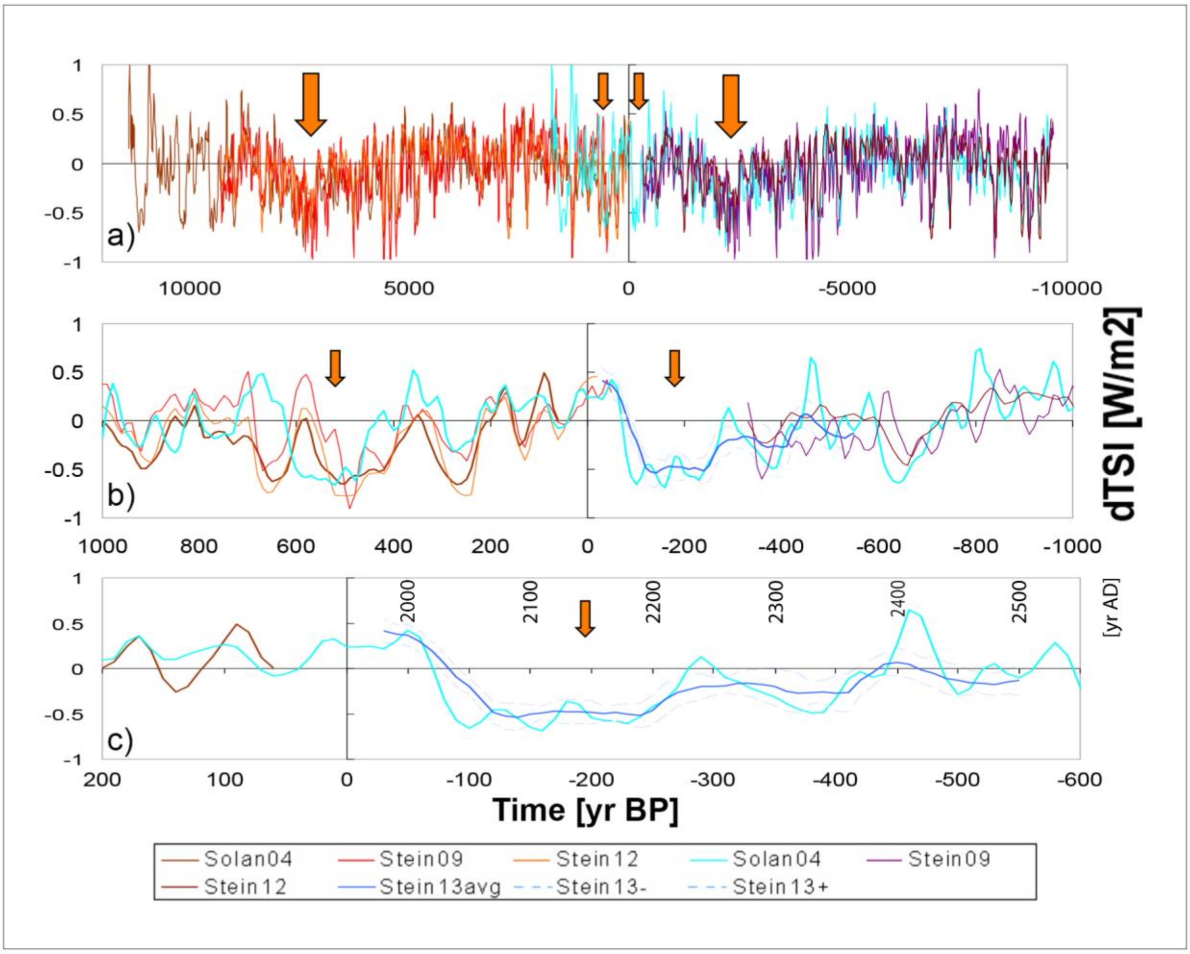
a)
b)
c)
dTSI [W/m2]
Time [yr BP]
[yr AD]
10000
5000
0
-5000
-10000
1000
800
600
400
200
-200
-400
-600
-800
-1000
100
-100
-300
-500
2000
2100
2200
2300
2400
2500
Solan04
Stein09
Stein12
Solan04
Stein09
Stein12
Stein13avg
Stein13-
Stein13+

Figure 4.